On the kinetics of the Langmuir-type heterogeneous reactions

Vladas Skakauskas, Pranas Katauskis[1]

Faculty of Mathematics and Informatics, Vilnius University
LT-03225 Vilnius, Lithuania
vladas.skakauskas@maf.vu.lt; pranas.katauskis@mif.vu.lt

Abstract. In this paper we investigate three two-dimensional in space mathematical models of the kinetics of unimolecular heterogeneous reactions proceeding onto planar surfaces. All models include the diffusion of the reactant from a bounded vessel towards an adsorbent, adsorption of the molecules of the reactant, their desorption, conversion (reaction) of the adsorbate into a product, instantaneous product desorption, and the diffusion of the product from the adsorbent into the same vessel. One of these models is based on the Langmuir-type kinetics of the surface reactions, the other one is based on the local steady-state value of the surface coverage, and the last one, in addition to the first model, involves the diffusion of the adsorbate along the adsorbent. Diffusivity of all species is assumed to be constant.

Models were solved numerically by using the finite difference technique. By changing input parameters the effects of the rate constants of the reactant adsorption, desorption, and reaction and the influence of the surface diffusion of the adsorbate and approximation of the surface coverage by its steady-state value on the kinetics of surface reactions were studied numerically.

Keywords: adsorption, desorption, heterogeneous reactions, unimolecular reactions, diffusion.

1 Introduction

Catalytic reactions proceeding on the surface of a solid or liquid (adsorbent) include the bulk diffusion of a reactant towards the adsorbent, adsorption of the reactant molecules onto the adsorbent, conversion (reaction) of the adsorbed molecules (adsorbate) into a product, desorption of the product from the adsorbent, and diffusion of the product away from the adsorbent. A part of the adsorbed molecules can desorb from the adsorbent. Adsorption is operative in most natural physical, biological, and chemical systems and is widely used in industrial applications. Being heterogeneous the kinetics of these processes depends on numerous different parameters. In solution the rate of these processes depends on the diffusivity of the reactant. At the interface this rate depends on the interaction forces between the adsorbed molecules of the reactant and surface. Molecules of the

---

[1]Corresponding author.

reactant that are physisorbed are adhered to the surface only through Van der Waals (weak intermolecular) interactions and can diffuse along the surface before the conversion into the product. Molecules of the reactant that are chemisorbed are adhered to the adsorbent through the formation of a chemical bond and cannot diffuse along the surface. They turn into the product directly. The simplest adsorption process is the Langmurian adsorption process in which no interactive forces between the adsorbate molecules are assumed and only monolayers are assumed to be formed. Kinetics of Langmuirian adsorption onto planar, spherical, and cylindrical surfaces is studied in [1]. In this case of surfaces the problem is one-dimensional and the assumptions that density of active centers of a surface is constant, an adsorbate cannot diffuse along the surface, and the pool of the reactant diffusing towards the adsorbent is large enough (i.e., the *volume of a vessel* containing the reactant is *infinite*) let authors of this paper to derive a nonlinear Volterra-type integral equation for the surface coverage, which they solved numerically. In [1], it is also given a survey of papers devoted to diffusion limited adsorption process in which the adsorption process is assumed to be very fast compared with the transport rate by diffusion. In the case where density of a reactant at the surface is given, the unimolecular reaction in a supported catalyst including desorption and the surface diffusion of the adsorbed molecules is studied [2]. In the same case where density of a reactant at the surface is given unimolecular, bimolecular, and trimolecular reactions proceeding on the surfaces with the heterogeneous distribution of the active centers are studied in [3–5] by using Monte Carlo simulations.

Monte Carlo simulations are also used to study a trimolecular surface reaction $2A+B_2 \rightarrow 2AB$ occurring on supported catalyst particles of the nanometer scale in [6–8] including monomolecular A adsorption on the support and its surface diffusion along the support, dissociative B_2 adsorption to the catalyst, and the Langmuir–Hinshelwood mechanism resulting in the formation of AB on the catalyst.

A common feature of the previous reports dealing with adsorption and surface reactions is that the desorption of the product is assumed to be instantaneous.

The existence and uniqueness theorems for models neglecting the surface diffusion of the adsorbate and product and including instantaneous or slow desorption of the product are given in [9] and [10]. Some results of numerical solving of the same models are discussed in [11]. Four models that include a slow product desorption and the surface diffusion of at least one of the adsorbate and product or neglect the surface diffusion are examined numerically in [12].

In the present paper we consider two-dimensional in space three one-molecular reaction models. All these models include the reactant diffusion towards the planar adsorbent from a *bounded vessel*, its adsorption onto and desorption from the adsorbent, the conversion of the adsorbate into a product, *instantaneous desorption of the product* and its diffusion away from the adsorbent. One of the models is based on the Langmuir-type kinetics, the other one is based on the steady-state approximation of the equation for the surface coverage, and the last one, in addition to the first model, involves the diffusion of the adsorbate along the adsorbent. We also assume that the diffusivity of all species is constant. The aim of this study is to estimate effects of the rate constants of the reactant adsorption, desorption and reaction and the influence the influence of the surface diffusion

of the adsorbate and the approximation of the surface coverage by its steady-state value on the kinetics of the catalytic reaction. To do this we solved all models numerically by using the finite difference technique. As is mentioned above, some numerical results of the first model is given in [11].

This paper is organized as follows. In Section 2 we give the formulation of the problem. Numerical results are discussed in Section 3. Section 4 concludes the paper.

2 Formulation of the problem

Suppose that reactant A and product B occupy a bounded domain $\Omega \subset \mathbb{R}^3$ with a surface $\partial\Omega = S_1 \cup S_2$, where S_2 is a part of $\partial\Omega$ (surface of the adsorbent) of the same dimension and $S_1 = \partial\Omega \setminus S_2$ is impermeable for A and B.

First we consider the case where the adsorbed molecules cannot diffuse along the adsorbent. Let $a(t, x)$ and $b(t, x)$ be the concentrations of reactant A and product B at time t at the position $x \in \Omega$ and $a_0(x)$ and $b_0(x)$ their initial distributions.

Then according to Langmuir [13], the adsorption, desorption, and reaction rates can be described by $k_f s (1 - \theta) a$, $k_r s \theta$, and $k s \theta$. Here s is a concentration of the active sites of S_2 that bind molecules of A, $\theta(t, x)$ is a fraction of s occupied by adsorbed molecules of A at time t at the position $x \in S_2$, $s(1 - \theta(t, x))$ is the concentration of the unoccupied active sites of S_2, $a(t, x)$ is the concentration of A at time t at the position $x \in S_2$, and k_f, k_r, and k are rate constants for the adsorption, desorption, and reaction, respectively. Hence, we have the kinetics equation for θ,

$$\begin{cases} \partial_t \theta = k_f (1 - \theta) a - (k_r + k)\theta, & t > 0, \ x \in S_2, \\ \theta(0, x) = \theta_0(x), & x \in S_2, \end{cases} \tag{1}$$

where $\partial_t \theta$ is the partial derivative of θ and $\theta_0(x)$ is the initial distribution of θ.

The diffusion of A and B can be described by the systems

$$\begin{cases} \partial_t a = \kappa_a \Delta a, & t > 0, \ x \in \Omega, \\ \partial_n a = 0, & t > 0, \ x \in S_1, \\ \kappa_a \partial_n a = -k_f s (1 - \theta) a + k_r s \theta, & t > 0, \ x \in S_2, \\ a(0, x) = a_0(x), & x \in \Omega \end{cases} \tag{2}$$

and

$$\begin{cases} \partial_t b = \kappa_b \Delta b, & t > 0, \ x \in \Omega, \\ \partial_n b = 0, & t > 0, \ x \in S_1, \\ \kappa_b \partial_n b = k s \theta, & t > 0, \ x \in S_2, \\ b(0, x) = b_0(x), & x \in \Omega, \end{cases} \tag{3}$$

where κ_a and κ_b are the diffusion coefficients of A and B, Δ is the Laplace operator, and $\partial_n a$ and $\partial_n b$ are the outward normal derivatives of a and b. Eqs. (1)–(3) represent the first model.

In the case where $|\partial_t \theta|$ is small, we can neglect it in Eq. (1) and get the formula for the steady-state value of θ,

$$\theta = \frac{k_f a}{k_f a + k_r + k}. \tag{4}$$

Then excluding θ from Eqs. (2) and (3) we get the other model,

$$\begin{cases} \partial_t a = \kappa_a \Delta a, & t > 0, \ x \in \Omega, \\ \partial_n a = 0, & t > 0, \ x \in S_1, \\ \kappa_a \partial_n a = -\dfrac{s k_f k a}{k_f a + k_r + k}, & t > 0, \ x \in S_2, \\ a(0, x) = a_0(x), & x \in \Omega \end{cases} \tag{5}$$

and

$$\begin{cases} \partial_t b = \kappa_b \Delta b, & t > 0, \ x \in \Omega, \\ \partial_n b = 0, & t > 0, \ x \in S_1, \\ \kappa_b \partial_n b = \dfrac{s k_f k a}{k_f a + k_r + k}, & t > 0, \ x \in S_2, \\ b(0, x) = b_0(x), & x \in \Omega, \end{cases} \tag{6}$$

with nonlinear boundary conditions.

At last in the case, where molecules of A are physisorbed, they can diffuse along S_2. In this case, Eqs. (1) have to be replaced by the system

$$\begin{cases} \partial_t \theta = k_f(1-\theta)a - (k_r + k)\theta + \kappa_\theta \Delta \theta, & t > 0, \ x \in S_2, \\ \partial_n \theta = 0, & t > 0, \ x \in \partial S_2, \\ \theta(0, x) = \theta_0(x), & x \in S_2, \end{cases} \tag{7}$$

where ∂S_2 is the contour which restricts S_2 and the constant κ_θ is the diffusion coefficient. Eqs. (7)-(2)-(3) present the third model to be considered in this paper.

If we integrate Eq. $(1)_1$ over S_2, Eqs. $(2)_1$ and $(3)_1$ over Ω, and use boundary and initial conditions of these systems, we get the mass conservation law,

$$\int_\Omega \big(a(t, x) + b(t, x)\big)\, dx + \int_{S_2} \theta(t, x)\, dx = \int_\Omega \big(a_0(x) + b_0(x)\big)\, dx + \int_{S_2} \theta_0(x)\, dx. \tag{8}$$

Similarly we derive the mass conservation law for system (5) and (6),

$$\int_\Omega \big(a(t, x) + b(t, x)\big)\, dx = \int_\Omega \big(a_0(x) + b_0(x)\big)\, dx. \tag{9}$$

Using the dimensionless variables $\bar{t} = t/T$, $\bar{x}_1 = x_1/l$, $\bar{x}_2 = x_2/l$, $\bar{a} = a/a_*$, $\bar{b} = b/a_*$, $\bar{a}_0 = a_0/a_*$, $\bar{b}_0 = b_0/a_*$ and constants $\bar{s} = s/a_* l$, $\bar{k}_f = k_f T a_*$, $\bar{k}_r = k_r T$, $\bar{k} = kT$, $\bar{\kappa}_a = \kappa_a T/l^2$, $\bar{\kappa}_b = \kappa_b T/l^2$, $\bar{\kappa}_\theta = \kappa_\theta T/l^2$, where T, l, and a_* are the characteristic dimensional units, we rewrite Eqs. (1)–(7) in the same form with t, x_1, x_2, a, b, a_0, b_0, k_f, k_r, k, s, κ_a, κ_b, and κ_θ replaced by $\bar{t}$, $\bar{x}_1$, $\bar{x}_2$, $\bar{a}$, $\bar{b}$, $\bar{a}_0$, $\bar{b}_0$, $\bar{k}_f$, $\bar{k}_r$, $\bar{k}$, $\bar{s}$, $\bar{\kappa}_a$, $\bar{\kappa}_b$, and $\bar{\kappa}_\theta$. For simplicity in what follows, we omit the bar and treat Eqs. (1)–(7) as dimensionless.

3 Numerical results

Mathematical models (1)–(3), (7)-(2)-(3), and (4)–(6) of the catalytic heterogeneous re-actions have been defined as initial boundary value problems based on a system of partial differential equations with complex nonlinear boundary conditions on S_2. Because of the complexity of the problem these systems cannot be solved analytically. Therefore, these problems were solved numerically by applying the method of finite differences together with the method of alternating directions [14].

Two-dimensional domain $\Omega = [0,1] \times [0,1]$ with $S_2 = \{(x_1, x_2)\colon x_1 \in [0,1],$ $x_2 = 0\}$ was discretized using a uniform grid. The constant steps $h_1 = h_2 = 0.01$ and $\tau = 0.01$ were used in the space directions x_1, x_2 and in the time direction, respectively. To approximate the differential problem (2) and (3) the alternating direction implicit method was used. The finite difference approximation of problem (1)–(3) was presented in [11]. The difference schemes to problems (5) and (6) differs from difference schemes to (2) and (3) by approximations of the boundary conditions at $x_2 = 0$ only. The explicit difference scheme to problem (1) and the implicit scheme to problem (7) were constructed taking into account discretizations of parabolic equations for a and b and approximations of the boundary conditions on S_2. We prove that the discrete analogue of the mass con-servation law (8) or (9) follows from the difference equations provided that functions $a_0(x)$ and $b_0(x)$ satisfy the conditions $\partial_{x_2} a_0(x)|_{x_2=0;1} = 0$, $\partial_{x_2} b_0(x)|_{x_2=0;1} = 0$. From the physical point of view $a(t,x) \to 0$, $\theta(t,x_1) \to 0$, and $b(t,x) \to \int_\Omega a_0(x)\,\mathrm{d}x$ as $t \to \infty$. Calculations show that numerical solutions preserve this property.

The approximation of (1), (2), (5), (6) and (7) resulted in the systems of linear alge-braic equations with a tridiagonal matrix. These systems were solved effectively by using the elimination method [8]. The numerical simulation was carried out using a software developed by the authors in C++ programming language.

The computer simulation for different values of h_1, h_2, and τ show the stable be-havior of the numerical solution. The numerical results were compared with the results calculated by using the explicit finite-difference schemes. The calculations confirm the stability of these difference schemes provided that the grid parameters h_1, h_2, and τ satisfy the inequality $\tau \leq h^2/(4\kappa)$, where $h = \min(h_1, h_2)$ and $\kappa = \max(\kappa_a, \kappa_b, \kappa_\theta)$.

Our selection of the values of parameters was motivated by the values available in the literature [1] with the extended range to allow exploration and illustration of the various regimes that are possible in catalytic reactions. For all calculations we used the following values of data:

$$T = 1\,\mathrm{s}, \quad l = 10^{-1}\,\mathrm{cm}, \quad s = 10^{-11}\,\mathrm{mol\,cm^{-2}}, \quad a_* = 10^{-11}\,\mathrm{mol\,cm^{-3}},$$
$$k_f \in \left[10^9, 10^{11}\right]\,\mathrm{cm^3\,mol^{-1}\,s^{-1}}, \quad k_r, k \in \left[10^{-2}, 1\right]\,\mathrm{s^{-1}},$$
$$\kappa_a, \kappa_b \in \left[5 \cdot 10^{-7}, 10^{-3}\right]\,\mathrm{cm^2\,s^{-1}}, \quad \kappa_\theta \in \left[5 \cdot 10^{-3}, 5 \cdot 10^{-2}\right]\,\mathrm{cm^2\,s^{-1}}. \quad (10)$$

Values of s, k_f, k_r, and κ_a were used in [1]. We expect that the chosen values of parameters were representative enough to illustrate a rich variety of possible scenarios. Values of constants that we use are given in captions.

Results of numerical solution are presented in Figs. 1–5 for $\Omega = [0,1] \times [0,1]$, $S_2 = \{(x_1, x_2): x_1 \in [0,1], x_2 = 0\}$, $\kappa_a = \kappa_b = 0.1$, $s = 10$, $\theta_0 = b_0 = 0$, $a_0 = 20(\exp(-2x_1) - \exp(-2))/(1 - \exp(-2))$.

As we indicated in the Introduction, the main purpose of our study was to estimate the effects of the adsorption, desorption, and reaction rate constants, adsorbate surface diffusion, and approximation of the surface coverage by its steady-state value on the kinetics of unimolecular surface reactions. As such, plots are presented below to illustrate these effects.

The plots in Figs. 1(a), 2(a), 3(a) and 1(b), 2(b), 3(b) depict the dependence of the reactant and product concentrations $a(t, 0, x_2)$ and $b(t, 0, x_2)$, respectively, on the adsorption rate constant k_f (Fig. 1), reaction rate constant k (Fig. 2), and desorption rate constant k_r (Fig. 3). Depicted results in Figs. 1(a), 2(a), 3(a) demonstrate the decrease of the reactant concentration $a(t, 0, x_2)$ as rate constants k_f and k grow and the increase of $a(t, 0, x_2)$ as k_r grows. Figs. 1(a), 2(b), 3(b) show that $b(t, 0, x_2)$ increases as k_f and k grow and it decreases as k_r increases. From Fig. 2(b) we observe a strong dependence of $b(t, 0, x_2)$ on reaction rate constant k. The qualitative behavior of concentrations $a(t, 0, x_2)$ and $b(t, 0, x_2)$ can be observed from system (1)–(3) directly without its numerical solving.

Figs. 4(a), 4(b), and 4(c) depict function $\theta(t, x_1)$ determined by system (1)–(3), (7)-(2)-(3), and (4)–(6). Figs. 4(a) and 4(b) demonstrate a nonmonotonic behavior of $\theta(t, x_1)$ for all x_1, while the behavior of $\theta(t, x_1)$ determined by (4) and (5) is nonmonotonic only in the region near $x_1 = 1$. Comparing Figs. 4(a) and 4(b) we observe a strong dependence of $\theta(t, x_1)$ on surface diffusivity κ_θ.

Function $\theta(t, x_1)$ determined by systems (1)–(3) and (7)-(2)-(3) get maximum values $\theta(t(x_1), x_1)$, where $t(x_1)$ increases as x_1 grows. The dependance of maximum values $\theta(t(x_1), x_1)$ on x_1 is strong for system (1)–(3) and it is weak for system (7)-(2)-(3). For example, in the case were $k_f = 1$, $k_r = 0.01$, $k = 0.5$, $t(x_1) \in [1.05, 3.6]$, $\theta(t(x_1), x_1) \in [0.11, 0.32]$ for system (1)–(3) and $t(x_1) \in [1.51, 1.94]$, $\theta(t(x_1), x_1) \in [0.18, 0.19]$ for system (7)-(2)-(3) with $\kappa_\theta = 0.5$.

(a)   (b)
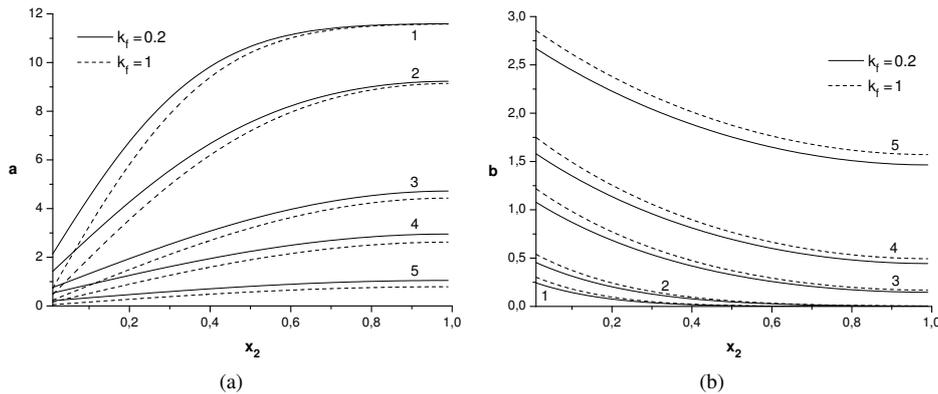
Fig. 1. Comparison of values of functions $a(t, 0, x_2)$ and $b(t, 0, x_2)$ determined by system (1)–(3) for two values of k_f and $k_r = 0.01$, $k = 0.05$. Values of time t: 0.5 (1), 1 (2), 3 (3), 5 (4), 10 (5).
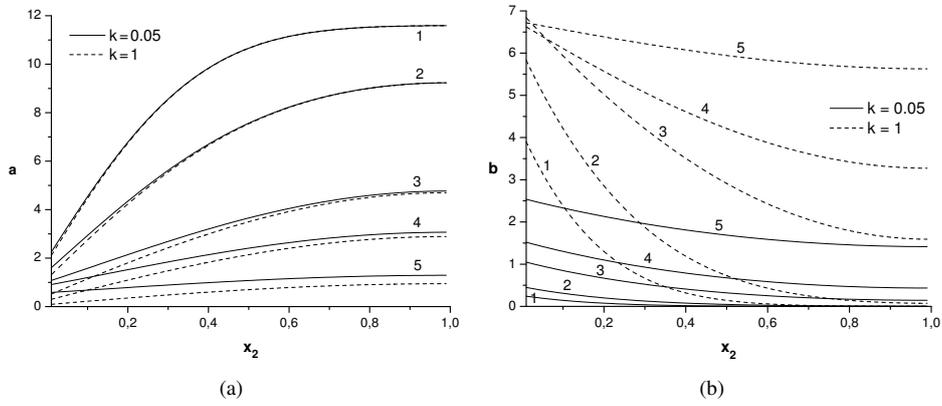
Fig. 2. Time evolution of $a(t, 0, x_2)$ and $b(t, 0, x_2)$ determined by system (1)–(3) for two values of k and $k_f = 0.2$, $k_r = 0.1$. Values of time are the same as in Fig. 1.
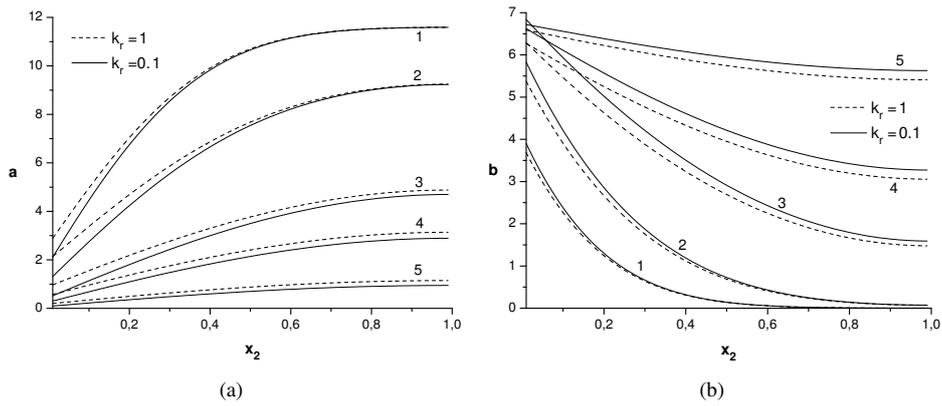
Fig. 3. Dependence of $a(t, 0, x_2)$ and $b(t, 0, x_2)$ determined by system (1)–(3) on k_r for $k_f = 0.2$, $k = 1$. Values of time are the same as in Fig. 1.
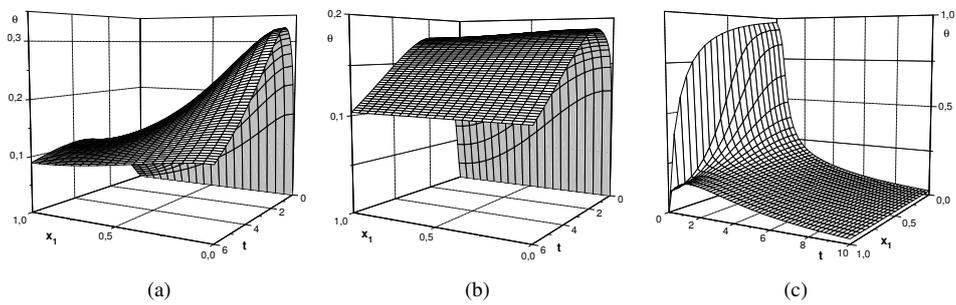
Fig. 4. Graphs of function $\theta(t, x_1)$ determined by systems (1)–(3) (a), (7)-(2)-(3) (b), and (4) and (5) (c) for $k_f = 1$, $k_r = 0.01$, $k = 0.5$.

(a)   (b)
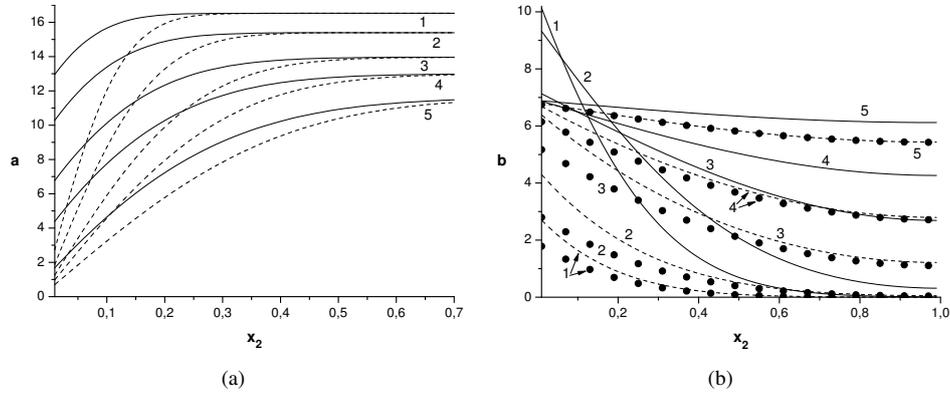
Fig. 5. Time evolution of $a(t, 0, x_2)$ and $b(t, 0, x_2)$ determined by systems (1)–(3)
(dashed line), (4)–(6) (solid line), and (7)-(2)-(3) with $\kappa_\theta = 0.5$ (bullets) for $k_f = 1$,
$k_r = 0.01$, $k = 0.5$. Values of time t: (a) 0.05 (1), 0.1 (2), 0.2 (3), 0.3 (4), 0.5 (5);
(b) 0.5 (1), 1 (2), 3 (3), 5 (4), 10 (5).

The plots in Fig. 5(a) depict the comparison of concentrations $a(t, 0, x_2)$ determined
by systems (1)–(3) and (4)–(6). Fig. 5(b) demonstrates the comparison of concentra-
tions $b(t, 0, x_2)$ determined by systems (1)–(3), (4)–(6), and (7)-(2)-(3). Concentrations
$a(t, 0, x_2)$ and $b(t, 0, x_2)$ determined by system (1)–(3) are larger than those determined
from system (7)-(2)-(3) and smaller than those determined from system (4)–(6). The
appreciable difference of concentration $a(t, 0, x_2)$ is observed near $x_2 = 0$ only for small
time (Fig. 5(a)). Difference of concentration $b(t, 0, x_2)$ is observed later in time, but it
vanishes for large time (Fig. 5(b)). Moreover, calculations show that in the region $x_2 = 0$
the difference between concentrations determined by systems (1)–(3) and (7)-(2)-(3) is
much smaller than that determined by system (4)–(6) and (1)–(3) or (4)–(6) and (7)-(2)-
(3). This result is natural since modulus of the flux of a at $t = 0$ and $x_2 = 0$ in system
(2) is larger than that in system (5), i.e.,

$$\left| \kappa_a \partial_n a(0, x_1, 0)|_{(2)} \right| = k_f s a_0(x_1) > k_f s a_0(x_1) \frac{k}{k_f a_0(x_1) + k_r + k}$$
$$= \left| \kappa_a \partial_n a(0, x_1, 0)|_{(5)} \right|.$$

Similarly, modulus of the flux of b at $t = 0$ and $x_2 = 0$ in system (3) is smaller than that
in system (6), i.e.,

$$\left| \kappa_b \partial_n b(0, x_1, 0)|_{(3)} \right| = 0 < k_f s a_0(x_1) \frac{k}{k_f a_0(x_1) + k_r + k}$$
$$= \left| \kappa_b \partial_n b(0, x_1, 0)|_{(6)} \right|.$$

Calculations also show that these inequalities preserve for small x_2 and $t > 0$.

4   Conclusion

Three two-dimensional in space mathematical models of the kinetics of unimolecular heterogeneous reactions occurring onto planar surfaces are examined numerically. All models include the diffusion of the reactant from a bounded vessel towards an adsorbent, adsorption of the molecules of the reactant, their desorption, conversion (reaction) of the adsorbate into a product, instantaneous product desorption, and the diffusion of the product from the adsorbent into the same vessel. One of these models is based on the Langmuir-type kinetics of the surface reactions, the other one is based on the approximation of the surface coverage by its local steady-state value, and the last one, in addition to the first model, involves the diffusion of the adsorbate along the adsorbent. Diffusivity of all species was constant.

Based on the present calculations, the following observations can be made:

- The increase of k_f decreases a, but increases b;

- The increase of k_r increases a, but decreases b;

- The increase of k decreases a, but increases b;

- Values of $a(t, 0, x_2)$ and $b(t, 0, x_2)$ from system (1)–(3) are smaller than those from system (4)–(6) and they are larger than values of $a(t, 0, x_2)$ and $b(t, 0, x_2)$ from system (7)-(2)-(3);

- Functions $\theta(t, x_1)$ from system (1)–(3) and (7)-(2)-(3) get maximum values $\theta(t(x_1), x_1)$, where $t(x_1)$ increases as x_1 grows. The dependence of maximum values $\theta(t(x_1), x_1)$ on x_1 is strong for system (1)–(3) and it is weak for system (7)-(2)-(3);

- Neglecting θ' in Eq. (1), i.e., using of Langmuir formula (4) leads to a significant difference between solutions to systems (4)–(6) and (1)–(3) or (7)-(2)-(3) in the region near the surface of the adsorbent for small time.

References

1. J. Kankare, I.A. Vinokurov, Kinetics of Langmurian adsorption onto planar, spherical, and cylindrical surfaces, *Langmuir*, **15**, pp. 5591–5599, 1999.

2. T.G. Mattos, F.D.A. Aarão Reis, Effects of diffusion and particle size in a kinetic model of catalyzed reactions, *J. Catal.*, **263**, pp. 67–74, 2009.

3. L. Cwiklik, B. Jagoda-Cwiklik, M. Frankowicz, Influence of spatial distribution of active centers on the kinetics of model heterogeneous catalytic processes, *Surf. Sci.*, **572**, pp. 318–328, 2004.

4. L. Cwiklik, B. Jagoda-Cwiklik, M. Frankowicz, Influence of the spacing between metal particles on the kinetics of reaction with spillover on the supported metal catalyst, *Appl. Surf. Sci.*, **252**, pp. 778–783, 2005.

5. L. Cwiklik, Influence of surface diffusion on catalytic reactivity of spatially inhomogeneous surfaces – mean-field modeling, *Chem. Phys. Lett.*, **449**, pp. 304–308, 2007.

6. V.P. Zhdanov, B. Kasemo, Kinetics of rapid heterogeneous reactions on the nanometer scale, *J. Catal.*, **170**, pp. 377–389, 1997.

7. V.P. Zhdanov, B. Kasemo, Monte Carlo simulation of kinetics of rapid reactions on nanometer catalyst particles, *Surf. Sci.*, **405**, pp. 27–37, 1998.

8. V.P. Zhdanov, B. Kasemo, Simulations of the reaction kinetics on nanometer supported catalyst particles, *Surf. Sci. Rep.*, **30**, pp. 25–104, 2000.

9. A. Ambrazevicius, Solvability of a coupled system of parabolic and ordinary differential equations, *Cent. Eur. J. Math.*, **8**, pp. 537–547, 2010.

10. A. Ambrazevicius, Existence and uniqueness theorem to a unimolecular heterogeneous catalytic reaction model, *Nonlinear Anal. Model. Control*, **15**(4), pp. 405–421, 2010.

11. V. Skakauskas, P. Katauskis, Numerical solving of coupled systems of parabolic and ordinary differential equations, *Nonlinear Anal. Model. Control*, **15**(3), pp. 351–360, 2010.

12. V. Skakauskas, P. Katauskis, Numerical study of the kinetics of unimolecular heterogeneous reactions onto planar surfaces, *J. Math. Chem.*, 2011 (in press).

13. I. Langmuir, The constitution and fundamental properties of solids and liquids. Part I. Solids, *J. Am. Chem. Soc.*, **38**, pp. 2221–2295, 1916.

14. A.A. Samarskii, *The Theory of Difference Schemes*, Marcel Dekker, New York, 2001.